Organic & Biomolecular Chemistry

Cite this: *Org. Biomol. Chem.*, 2012, **10**, 9383

www.rsc.org/obc

PAPER

Ortho-phenylenediamine-based open and macrocyclic receptors in selective sensing of $H_2PO_4^-$, ATP and ADP under different conditions†

Kumaresh Ghosh* and Indrajit Saha

Received 19th June 2012, Accepted 15th October 2012
DOI: 10.1039/c2ob26995c

Ortho-phenylenediamine-based open and macrocyclic receptors have been designed and synthesized. The open receptor **1** and the macrocyclic receptor **2** fluorimetrically distinguish $H_2PO_4^-$ from the other anions examined in CH_3CN with appreciable binding constant values. As practical applications, they are also sensible to nucleotides in aq. CH_3CN (1 : 1, v/v). The receptor **1** shows significant emission change upon complexation of ATP and ADP. ADP is selectively distinguished by a ratiometric change in emission. In contrast, the macrocyclic receptor **2**, under similar conditions, shows good binding with ATP over the others.

Introduction

The design and synthesis of fluorescent receptors of simple architectures for sensing anions of different shapes is an area of interest to the supramolecular chemists.[1] Anions are omnipresent in biological systems and play important roles in biology, pharmacy and environmental sciences.[2] Among the different anions, phosphate anions (both inorganic and organic) are important as they take part in almost all metabolic processes.[3] On the other hand, phosphate derivatives encompassing nucleotides (ATP, ADP and AMP) are equally important for their role in bioenergetics, metabolism, and transfer of genetic information.[4] For instance, ATP is a multifunctional nucleotide, important as a molecular currency of intracellular energy transfer, and is also involved in DNA replication and transcription.[5] ADP and AMP are the hydrolysis products of ATP under cellular conditions and therefore the ratio of ATP to AMP is useful in giving the information on the metabolic rate of the cell. ATP also serves as a phosphate donor in kinase catalysed protein phosphorylation. Deficiency in ATP results in ischemia, Parkinson's disease, and hypoglycemia.[5f] Therefore, selective sensing of any one of these nucleotides (ATP, ADP and AMP) and also the inorganic phosphate either in the form of $H_2PO_4^-$ or PO_4^{3-} is challenging. Considerable effort has been devoted to recognising such species by synthetic fluororeceptors. To date various fluorescent receptors for dihydrogenphosphate ($H_2PO_4^-$)[6] as well as for nucleotide[7] (*e.g.*, ATP, ADP and AMP) recognition have been reported in the literature.

In continuation of our interest to develop *ortho*-phenylenediamine-based synthetic clefts for the selective sensing of anions,[6k,7m,8] we report here two new receptor modules **1** and **2** that selectively recognize tetrabutylammonium dihydrogenphosphate in CH_3CN over a series of other anions by exhibiting characteristic emissions. In addition, both the receptors are sensitive to the detection of ATP and ADP in aq. CH_3CN (1 : 1, v/v) with distinguishable features.

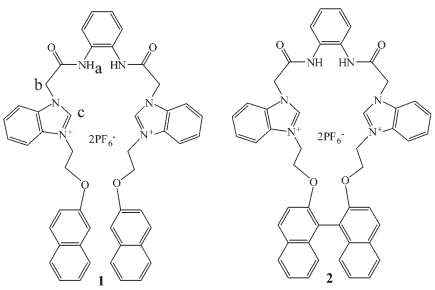

Results and discussion

The receptors **1** and **2** were accomplished according to Schemes 1 and 2. In Scheme 1, 2-naphthol was transformed into the chloro compound **4b**, which on reaction with benzimidazole in the presence of NaH gave compound **5**. Further reaction of **5** with the compound **3**, obtained from the reaction of *ortho*-phenylenediamine with chloroacetyl chloride, furnished dichloride salt **6**. Exchange of Cl^- in **6** with NH_4PF_6 yielded the compound **1** in appreciable yield.

The macrocycle **2** was synthesized following the reaction in Scheme 2. Initially, (*rac*)-1,1′-binaphthol (BINOL) **7** was

Department of Chemistry, University of Kalyani, Kalyani-741235, India. E-mail: ghosh_k2003@yahoo.co.in; Fax: +913325828282; Tel: +913325828750

† Electronic supplementary information (ESI) available: Figures showing the change in fluorescence and UV-vis titrations of receptors **1** and **2** with various anions, Job plot, NMR and mass spectra and other figures of **1** and **2**. See DOI: 10.1039/c2ob26995c

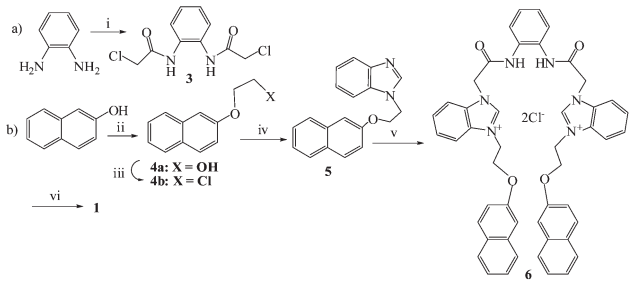

Scheme 1 (a) i. Chloroacetyl chloride, Et_3N, dry CH_2Cl_2, 1 h, 91%; (b) ii. 2-Chloroethanol, K_2CO_3, acetone, reflux 24 h, 67%; iii. $SOCl_2$, dry pyridine (cat.), dry $CHCl_3$, 12 h, 91%; iv. Benzimidazole, NaH, TBAI, dry THF, reflux 10 h, 86%; v. **3**, dry CH_3CN, reflux, 5 days, 64%; vi. NH_4PF_6, DMF–H_2O (1 : 1, v/v), $\frac{1}{2}$ h, 90%.

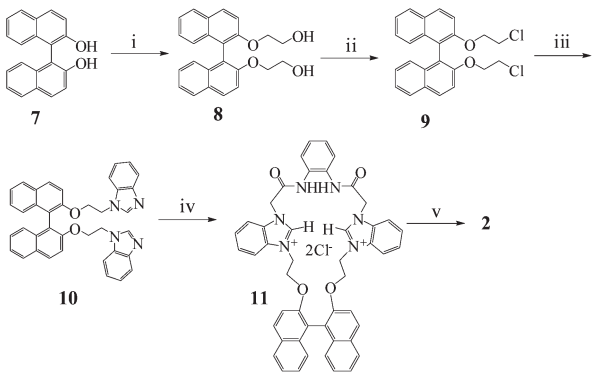

Scheme 2 i. 2-Chloroethanol, K_2CO_3, acetone, reflux 24 h, 65%; ii. $SOCl_2$, pyridine (cat.), dry $CHCl_3$, 12 h, 81%; iii. Benzimidazole, NaH, TBAI, dry THF, reflux 10 h, 42%; iv. **3**, dry CH_3CN (high dilution), reflux, 4 days, 69%; (v) CH_3OH–H_2O, NH_4PF_6, 30 min, 87%.

refluxed with 2-chloroethanol in dry acetone in the presence of K_2CO_3 to afford compound **8**. It was next treated with $SOCl_2$ in dry $CHCl_3$ to obtain the dichloro compound **9**, which on reaction with benzimidazole in the presence of NaH gave compounds **10**. High dilution reaction of **10** with the compound **3** in dry CH_3CN under refluxing conditions produced the dichloride salt **11**. The anion exchange of **11** using NH_4PF_6 in CH_3OH afforded compound **2** in 87% yield.

Anion binding studies

Anion binding properties of **1** towards a series of anions were evaluated using UV-vis, and fluorescence titration experiments. Additionally, ^1H NMR spectra were recorded in the presence of the anionic guests to identify the interacting protons in the binding domain of **1**. In fluorescence, the receptor **1** ($c = 3.75 \times 10^{-5}$ M) showed emission at 345 nm when excited at 300 nm in CH_3CN. Upon titration with $H_2PO_4^-$, the emission intensity at 345 nm increased with a red shift of ~15 nm (Fig. 1a) followed by the appearance of broad structured emission centered at 420 nm. We believe that this broad, structured emission arises from the energetically and structurally distinct isomers of the excimer complex (that probably would exist only at the excited state). In general, as most of the possible excited state isomers

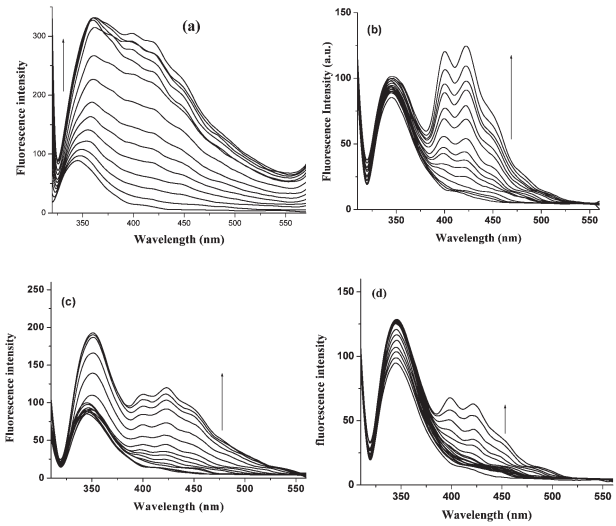

Fig. 1 Change in emission of receptor **1** ($c = 3.75 \times 10^{-5}$ M) in CH_3CN with increase in concentration of (a) $H_2PO_4^-$, (b) ClO_4^-, (c) F^- and (d) AcO^- upon excitation at 300 nm.

are isoenergetic to each other, we see one broad excimer peak. However, the major contribution to the broad peak is due to the relaxation from different vibrational levels of the excited state to the ground state. In this case, there could be different distinct excimer complexes which may give rise to structured broad emission.[9] Such a structured nature of the excimer emission was more clearly observed in titration spectra of **1** with ClO_4^-, F^- and AcO^- (Fig. 1b–1d), keeping the monomer maxima almost unaltered at 345 nm, except for F^-. A nearly 5 nm red shift of the monomer emission was noticed with F^-. The change in fluorescence intensity of **1** with the other anions was too small to consider effective complexation (Fig. S1 in ESI†). As can be seen from Fig. 2, the change in fluorescence ratio at 345 nm in the presence of 3 equivalent amounts of anions is significant only for $H_2PO_4^-$. Upon addition of 3 equivalent amounts of the anions, the excimer emission was not much intense except in the case of $H_2PO_4^-$. Therefore, the titration was further continued up to the addition of 10 equivalent amounts of the guests. The growth of the excimer was noted to be significant upon the addition of F^-, ClO_4^-, and $H_2PO_4^-$ (Fig. S5, ESI†). The associated change in ratio of the excimer emission to monomer emission with [G]/[H] is highlighted in Fig. S6 (ESI†). The downward running of the curve for $H_2PO_4^-$ in Fig. S6† is attributed either to decomplexation or the deprotonation of the bound $H_2PO_4^-$ ions.[10]

The complexation induced enhancement of fluorescence in **1** is explained due to the deactivation of the thermodynamically favorable PET process occurring in between the binding site and the excited state of naphthalene.

However, the sharp break of the titration curves at [G]/[H] = 1 for AcO^- and $C_6H_5COO^-$ with **1** (Fig. S7, ESI†) and at [G]/[H] = 2 with $H_2PO_4^-$, fumarate demonstrates the formation of 1 : 1 and 2 : 1 (guest : host) complexes, respectively. Job plots[11] further confirmed this except in the case of $H_2PO_4^-$. The exact stoichiometry of the complex of $H_2PO_4^-$ with **1** was evaluated to be 1 : 1 from Job's plot (Fig. S8, ESI†).

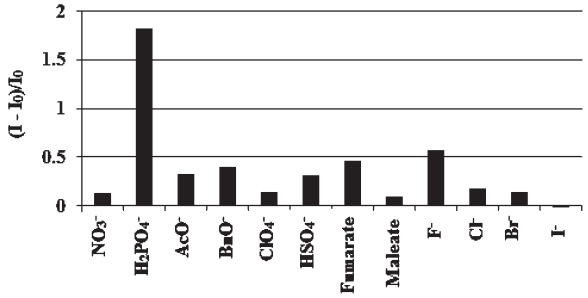

Fig. 2 Fluorescence ratio ($I - I_0/I_0$) of receptor **1** ($c = 3.75 \times 10^{-5}$ M) at 345 nm upon addition of 3.0 equivalent amounts of a particular anion in CH_3CN.

Time resolved fluorescence measurement of **1** ($\lambda_{exc} = 300$ nm) was carried out in the presence and absence of anions such as $H_2PO_4^-$ and ClO_4^-. The emission decay profile of **1** monitored at 345 nm could be fitted bi-exponentially with two constants $\tau_1 = 0.224$ ns (91.11%), $\tau_2 = 7.07$ ns (8.89%). The faster decay component (0.224 ns) is due to the benzimidazolium moiety and a relatively stable component with greater lifetime (7.07 ns) is attributed to the naphthalene motif of **1**. In the presence of 1 equivalent amount of $H_2PO_4^-$, while the lifetime of the benzimidazolium moiety marginally increases (0.247 ns, 47.63%), the lifetime for the naphthalene motif decreases significantly (1.78 ns, 52.37%). Between these two, the component 1.78 ns for naphthalene with nearly the same preexponential factor as that of the benzimidazolium motif is substantially destabilized due to complexation of $H_2PO_4^-$ into the benzimidazolium sites of **1**. Complexation at this site induces a conformational change for which the naphthalene groups come close to form the excimer. This is established from the emission decay profile of **1** at the excimer wavelength (420 nm) in the presence of an equivalent amount of $H_2PO_4^-$. The bi-exponential emission decay profile of **1**·$H_2PO_4^-$ monitored at the excimer wavelength (420 nm) reveals that the contribution of this component towards the total emission is significantly greater (5.14 ns, 91.42%). Like $H_2PO_4^-$, ClO_4^- anion binding also affected the decay profile of **1**. The bi-exponential fluorescence decay profile of the complex **1**·ClO_4^- at the monomer emission wavelength (345 nm) corroborates that the contribution of the component for the naphthalene motif towards total emission is considerably small (5.9 ns, 9.21%) compared to the short-lived component assigned to the benzimidazolium motif (0.25 ns, 90.79%). This is quite different from the situation as observed for the complex of **1**·$H_2PO_4^-$. The results are accumulated in Table 1 and the decay profiles are represented in Fig. S9 and S10 (ESI†).

In order to investigate the ground state binding of **1**, UV-vis titration experiments were carried out in CH_3CN (Fig. S3, ESI†). Except for $H_2PO_4^-$ and F^-, the anion binding induced change in absorbance for the naphthalene moiety (~320 nm) in **1** was minor with anions such as Cl^- and NO_3^- (Fig. S3, ESI†). As noted in Fig. S3,† the greater change in absorbance at 269 nm for the benzimidazolium moiety relative to the naphthalene moiety explains the weak interaction of the cleft of **1** with the anions in the ground state. Accordingly, we were unable to determine the binding constant values for the anions considering the absorbance data. Indeed, we determined the binding constants for **1** with the anions using the fluorescence data (Table 2).[12a] It is evident from Table 2 that the open cleft of **1** has a preference for the $H_2PO_4^-$ ion, although other anions exhibit moderate binding.

The selectivity in the binding of $H_2PO_4^-$ by **1** was confirmed from the change in emission of **1** in the presence of other anions. Fig. 3 describes this aspect. Only F^- shows some interference in the binding process.

Table 1 Fluorescence decay times (τ), and preexponential factors for **1** in CH_3CN

Receptor in the presence and absence of guest	Fluorescence decay time τ (preexponential factor)
1 at 345 nm	$\tau_1 = 2.24 \times 10^{-10}$ (91.11%), $\tau_2 = 7.07 \times 10^{-9}$ (8.89%) ($\chi^2 = 1.04$)
1 + $H_2PO_4^-$ at 345 nm	$\tau_1 = 2.47 \times 10^{-10}$ (47.63%), $\tau_2 = 1.78 \times 10^{-9}$ (52.37%) ($\chi^2 = 1.03$)
1 + $H_2PO_4^-$ at 420 nm	$\tau_1 = 3.87 \times 10^{-10}$ (8.58%), $\tau_2 = 5.14 \times 10^{-9}$ (91.42%) ($\chi^2 = 1.11$)
1 + ClO_4^- at 345 nm	$\tau_1 = 2.5 \times 10^{-10}$ (90.79%), $\tau_2 = 5.9 \times 10^{-9}$ (9.21%) ($\chi^2 = 1.08$)

Table 2 Association constant values for receptor **1**

Anions	K_a in M^{-1} at 422 nm
$H_2PO_4^-$	1.23×10^4
Fumarate	nd
ClO_4^-	3.65×10^3
F^-	4.97×10^3
CH_3COO^-	1.85×10^3

nd = not determined.

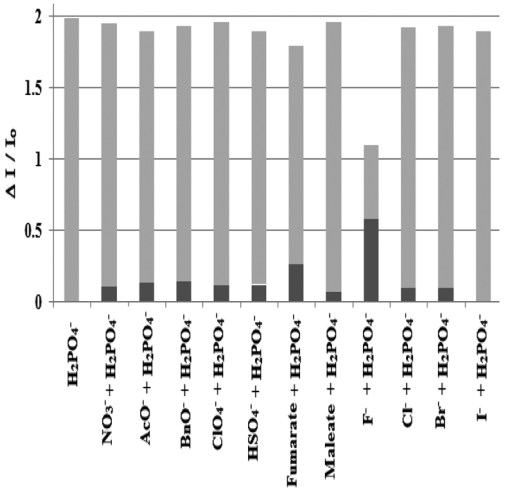

Fig. 3 Change in fluorescence ratio of **1** ($c = 3.75 \times 10^{-5}$ M) upon addition of 10 equivalent amounts of $H_2PO_4^-$ in the presence of other anions in CH_3CN.

The anion binding was also realized from ^{1}H NMR in CD_3CN. In this regard, Fig. S11 (ESI†) shows the change in ^{1}H NMR of **1** in the presence and absence of equivalent amounts of AcO^- and F^- anions. Upon addition of AcO^-, the amide protons (H_a), which appeared at 8.75 ppm, became too broad to detect. This may be due to either deprotonation or the hydrogen bonding effect. But the benzimidazolium protons (H_c) suffered a considerable downfield chemical shift ($\Delta\delta$ = 0.54 ppm) indicating their intimate hydrogen bonding contact with the carboxylate moiety. A similar finding was noted on addition of F^- to the solution of **1** in CD_3CN. Interestingly, the methylene protons of type b underwent downfield shifts by 0.13 to 0.21 ppm upon complexation of both AcO^- and F^- ions. However, addition of equivalent amounts of $H_2PO_4^-$ to **1** in CD_3CN resulted in precipitation. But we were successful in recording ^{1}H NMR of the complex of **1** with $H_2PO_4^-$ in DMSO-d_6 which is known as a hydrogen bonding interfering solvent in host–guest complexation.[13] In this regard, the spectral change for **1** with $H_2PO_4^-$ is shown in Fig. 4. The results for AcO^- and F^- can be found in Fig. S12 (ESI†). With $H_2PO_4^-$ the change in the chemical shift of the interacting protons of **1** was considerable and the binding constant value was determined to be 1.63×10^3 M^{-1}.[12b] This is less compared to the value obtained by the fluorescence method in less polar CH_3CN. For other anions, small shifting of the interacting amide and benzimidazolium protons due to significant interference of DMSO was the main hindrance to determining the binding constant values accurately.

Based on observations in ^{1}H NMR and emission studies (see Fig. 1), we proposed binding structures of **1** with AcO^-, $H_2PO_4^-$, F^- and ClO_4^- ions which were optimized by the PM6 method[14] in CH_3CN solvent (Fig. 5). As can be seen from Fig. 5, F^- and ClO_4^- ions are complexed into the cavity involving less hydrogen bonds. The fluoride ion being smaller in the series does not fit into the cavity properly. Even though the change in emission of **1** in the presence of F^- is attributed to its more basic character that regulates hydrogen bond formation and deprotonation of the benzimidazolium and amide protons during the event. On complexation the pendant naphthalene groups under flexible linkers are stacked either in edge-to-face or face-to-face mode. This is in accordance with the appearance of the excimer in Fig. 1.

To improve the selectivity in binding, the macrocyclic structure **2** ($c = 3.43 \times 10^{-5}$ M) which showed emission at 365 nm in CH_3CN on excitation at 300 nm was considered. Fig. 6 represents the change in emission of **2** upon addition of 2.0 equivalent amounts of various anions in CH_3CN and the emission intensity of the macrocycle is significantly perturbed in the presence of $H_2PO_4^-$ and fumarate only. Both the anions followed 2 : 1 (guest : host) binding stoichiometry, evident from the break of the titration curves in Fig. S13 (ESI†). Fig. 7a and 7b illustrate the emission titration spectra of **2** with $H_2PO_4^-$ and fumarate anions, respectively. During titration, the emission at 365 nm was red shifted by ~13 nm and ~11 nm with $H_2PO_4^-$ and fumarate anions, respectively. Here also the complexation induced

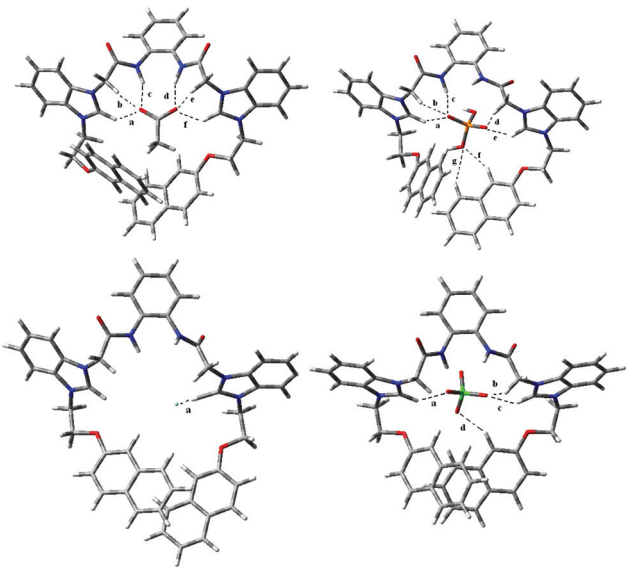

Fig. 5 PM6 optimized structures for **1** with (a) $H_2PO_4^-$ [a = 1.79 Å, b = 2.80 Å, c = 1.72 Å, d = 2.05 Å, e = 1.92 Å, f = 2.28 Å, g = 2.55 Å; $d_{nap-nap}$ = 3.12 Å], (b) AcO^- [a = 1.88 Å, b = 2.19 Å, c = 1.71 Å, d = 1.69 Å, e = 2.18 Å, f = 1.90 Å, $d_{nap-nap}$ = 2.76 Å], (c) F^- [a = 1.022 Å, $d_{nap-nap}$ = 3.89 Å] and (d) ClO_4^- [a = 1.99 Å, b = 2.16 Å, c = 2.07 Å, d = 2.44 Å, 2.55 Å, $d_{nap-nap}$ = 3.20 Å], in CH_3CN.

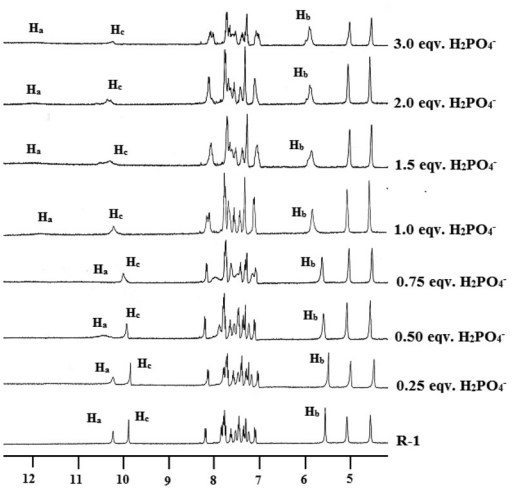

Fig. 4 Change in ^{1}H NMR (400 MHz) of **1** ($c = 2.67 \times 10^{-3}$ M) upon successive addition of tetrabutylammonium dihydrogenphosphate ($c = 6.76 \times 10^{-2}$ M) in d_6-DMSO.

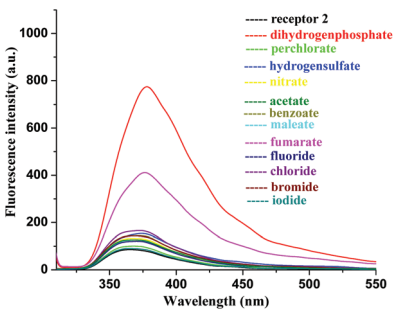

Fig. 6 Change in fluorescence intensity of **2** ($c = 3.43 \times 10^{-5}$) at 365 nm (λ_{Ex} = 300 nm) in the presence of 2 equivalent amounts of anions.

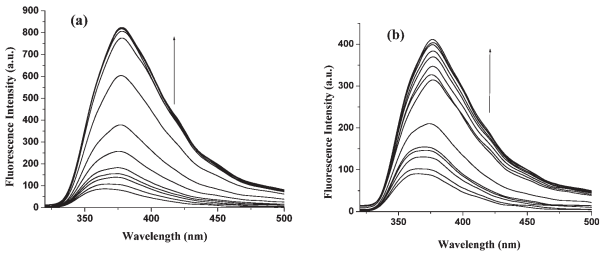

Fig. 7 Change in emission of receptor (a) **2** ($c = 3.43 \times 10^{-5}$ M) with increase in concentrations $H_2PO_4^-$ and (b) fumarate ($\lambda_{exc} = 300$ nm).

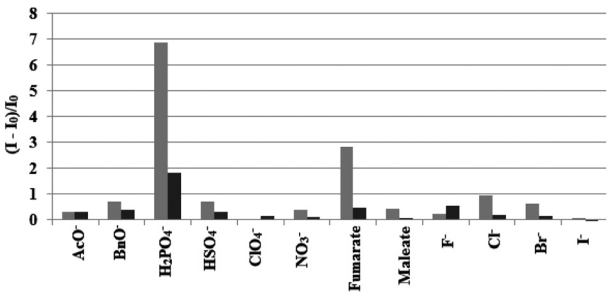

Fig. 8 Fluorescence ratio ($I - I_0/I_0$) of receptors **1** ($c = 3.75 \times 10^{-5}$ M) and **2** ($c = 3.43 \times 10^{-5}$ M) nm upon addition of 3.0 equivalent amounts of a particular anion in CH_3CN (grey color = receptor **2** and black color = receptor **1**).

Table 3 Fluorescence decay times (τ), and preexponential factors for **2** in CH_3CN

Receptor in the presence and absence of guest	Fluorescence decay time τ (preexponential factor)
2 at 365 nm	$\tau_1 = 1.36 \times 10^{-10}$ (20.19%), $\tau_2 = 5.1 \times 10^{-9}$ (79.81%) ($\chi^2 = 1.09$)
2 + $H_2PO_4^-$ at 365 nm	$\tau_1 = 2.53 \times 10^{-10}$ (17.68%), $\tau_2 = 3.0 \times 10^{-9}$ (82.32%) ($\chi^2 = 0.98$)

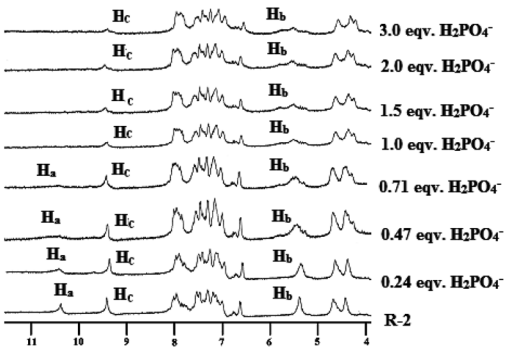

Fig. 9 Change in ^1H NMR (400 MHz) of **2** ($c = 2.85 \times 10^{-3}$ M) upon addition of tetrabutylammonium dihydrogenphosphate ($c = 6.76 \times 10^{-2}$ M) in d_6-DMSO.

increase in emission is assumed to be due to the deactivation of the PET (photo-induced electron transfer) process occurring in between the macrocyclic binding domain and the excited state of the BINOL fluorophore. However, other anions, except $H_2PO_4^-$ and fumarate, interacted weakly with the macrocycle **2** (Fig. S2, ESI†) in CH_3CN and it was difficult to determine the stoichiometries and association constants for them accurately. Fig. S14 (ESI†) describes the change in fluorescence ratio of **2** upon addition of 4.0 equivalent amounts of various anions. Fig. 8 illustrates the comparative views on the change in emission of the receptors **1** and **2** upon complexation of 3 equivalent amounts of each anion. The comparison interprets that the macrocycle **2** shows greater sensitivity and selectivity towards $H_2PO_4^-$ and fumarate anions in CH_3CN than the acyclic receptor **1**.

In the interaction process, the stoichiometries of the complexes of **2** with both $H_2PO_4^-$ and fumarate were established from Job's plots. In the case of $H_2PO_4^-$, an equilibrium mixture of both 1 : 1 and 1 : 2 (host : guest) types of complexes was noticed (Fig. S15a, ESI†). On the other hand, fumarate attained a sharp 1 : 1 stoichiometry (Fig. S15b, ESI†).

Time resolved fluorescence measurement was also performed with **2** ($\lambda_{exc} = 300$ nm) in the presence and absence of $H_2PO_4^-$ (Table 3). The emission decay profile of **2** monitored at 365 nm could be fitted bi-exponentially with two constants $\tau_1 = 0.136$ ns (20.19%), $\tau_2 = 5.1$ ns (79.81%) (Fig. S16, ESI†). The faster decay component (0.136 ns) is due to the benzimidazolium moiety and a relatively stable component with greater lifetime (5.1 ns) is attributed to the BINOL motif of **2**. However, in the presence of 1 equivalent amount of $H_2PO_4^-$, while the lifetime of the benzimidazolium moiety increases (0.253 ns, 17.68%), the lifetime for the BINOL motif decreases significantly (3 ns, 82.32%) (Fig. S16b, ESI†) and contributes to the total fluorescence with a greater preexponential factor compared to that of the benzimidazolium motif which is stabilized due to complexation of $H_2PO_4^-$ *via* hydrogen bonding and charge–charge interactions.

The ground-state binding of **2** was understood from UV-vis titration experiments in CH_3CN (Fig. S4, ESI†). The change in absorbance of **2** with increase in concentration of a particular anion was negligible or irregular suggesting weak interaction in the ground state. Therefore, we determined the association constant values[12a] for **2** with the anions (K_a for $H_2PO_4^-$ = 7.47 × 10^3 M^{-1} and K_a for fumarate = 3.71 × 10^3 M^{-1}) considering the emission data. The selectivity in the binding of $H_2PO_4^-$ by **2** was realized by observing the change in fluorescence ratio in the presence and absence of other anions (Fig. S17, ESI†). Only fumarate showed interference in the selectivity profile.

However, with a view to identifying the interacting protons of the macrocycle **2**, we tried to record ^1H NMR of **2** in the presence of equivalent amounts of $H_2PO_4^-$ and fumarate (taken as their tetrabutylammonium salts) in CD_3CN in the concentration range ~10^{-3} M. But we failed to record due to precipitation. Thus, like **1**, ^1H NMR titration of **2** with the anions was attempted in d_6-DMSO. Strong interference of DMSO hindered the interaction of anions into the macrocyclic cavity as confirmed by the small change in chemical shift in Fig. S18 (ESI†). Fig. 9 displays the spectral change for **2** with $H_2PO_4^-$ in d_6-DMSO where only a minor change in chemical shift values of benzimidazolium and amide protons is observed and the binding constant value was evaluated[12b] to be 4.0 × 10^2 M^{-1} which is less than the value obtained by the fluorescence method in less polar CH_3CN.

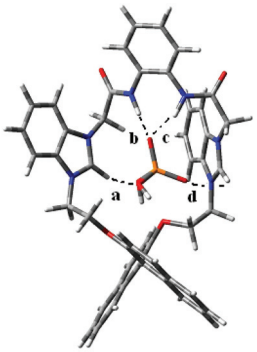

Fig. 10 PM6 optimized structure for **2** with $H_2PO_4^-$ (a = 2.06 Å, b = 1.77 Å, c = 1.71 Å, d = 2.17 Å) in CH_3CN.

The hydrogen bonding capability of **2** with $H_2PO_4^-$ was further understood from the PM6 optimized structure[14] in CH_3CN. Only the benzimidazolium and amide protons are involved in the complexation (Fig. 10).

In order to understand the recognition properties of compounds **1** and **2** towards the same anions in a semi-aqueous system, we further carried out the interaction study in CH_3CN–H_2O (1 : 1 v/v). Both **1** and **2** showed minor changes in emission spectra upon addition of the anions.

Complexation studies with biologically relevant phosphate anions

To explore the potential applications of both the receptors **1** and **2**, we further investigated the behaviour of these molecules with the sodium salt of seven biologically relevant phosphate anions such as ATP, ADP, AMP, $H_2PO_4^-$, HPO_4^{2-}, PO_4^{3-} and $P_2O_7^-$. In this context, a higher content of water in aqueous measuring solution was desirable, but such an approach was constrained due to the limited solubility of the receptors in water. As a reasonable negotiation, a 1 : 1 aqueous CH_3CN solution was used in the study.

The receptor **1** showed an emission band at 345 nm in CH_3CN–H_2O (1 : 1, v/v) when excited at 300 nm. The complexation induced change in fluorescence of **1** upon addition of 20 equivalent amounts of the anions is displayed in Fig. 11. It is clearly understood that receptor **1** has a preference for ATP and ADP over the other anions studied. Fig. 12a and 12b represent the emission titration spectra for **1** with ADP and ATP, respectively.

A closer look into the emission profiles reveals that on progression of the titration a new band at ~383 nm appears significant. We presume that this band, observed in the case of both ATP and ADP, is due to the complexation-induced unique sandwich π–π stacking interaction of naphthalene–adenine–naphthalene units as shown in Fig. 13 for ADP. Optimization of this suggested complex by the PM6 method in pure CH_3CN intimated a deviation (Fig. S21, ESI†). One of the naphthalenes resides close to the adenine nucleus of ADP. To know about the actual organization of the components, we tried to crystallize **1** with ADP and ATP in several combinations of organic solvents. But we were unsuccessful in obtaining good quality crystals for X-ray diffraction. Interestingly, though the emission at the higher

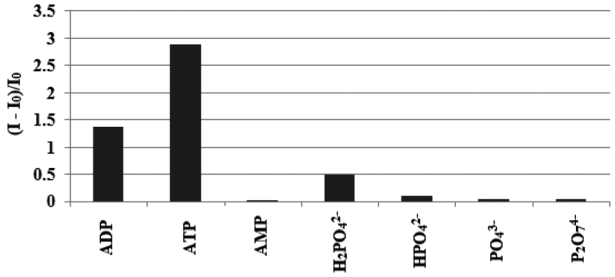

Fig. 11 Change in fluorescence ratio ($I - I_0/I_0$) of receptor **1** (c = 4.92 × 10^{-5} M) at 385 nm upon addition of 20 equivalents of a particular anion in CH_3CN–H_2O (1 : 1, v/v).

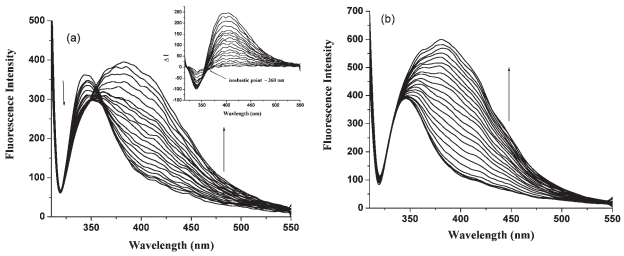

Fig. 12 Change in emission of receptor **1** (c = 4.92 × 10^{-5} M) with increase in concentration of (a) ADP [inset: difference spectra obtained upon addition of ADP against initial emission of **1**] and (b) ATP upon excitation at 300 nm in CH_3CN–H_2O (1 : 1, v/v).

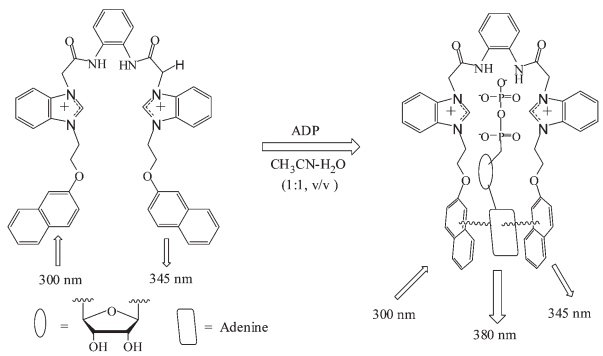

Fig. 13 Suggested binding structure of **1** with ADP.

wavelength for the excimer was observed upon complexation of both ADP and ATP, the change in monomer emission distinguished these two species effectively. In the case of fluorometric titration of **2** with ADP the monomer emission decreases and the excimer emission increases showing a ratiometric change with an isosbestic point at ~360 nm (inset Fig. 12a). To the best of our knowledge, till date, no ratiometric chemosensor for ADP is known in the literature. On the other hand, with increasing concentrations of ATP, both the monomer and excimer emissions of **1** gradually increase with a slight red shift. Stoichiometries of the complexes of **1** with ADP and ATP were 1 : 1 as confirmed by Job's plot (Fig. S22, ESI†).[11] Thus the receptor **1** shows selectivity towards ADP and ATP, and more importantly, it can fluorometrically discriminate ADP from other phosphates by showing a ratiometric change in emission.

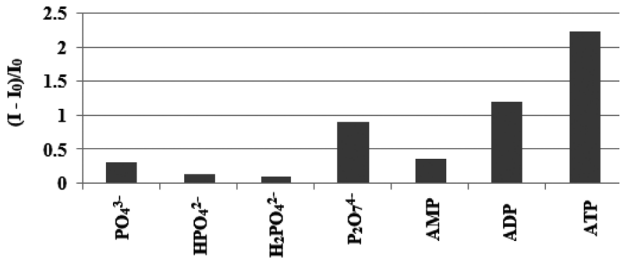

Fig. 14 Change in fluorescence ratio ($I - I_0/I_0$) of receptor **2** (c = 3.83 × 10^{-5} M) at 365 nm upon addition of 4.0 equivalents of a particular anion in CH_3CN–H_2O (1 : 1, v/v).

On the other hand, macrocycle **2** showed a well defined emission band at 365 nm when excited at 300 nm in CH_3CN–H_2O (1 : 1, v/v). Fig. 14 represents the change in fluorescence ratio of **2** upon addition of 4 equivalent amounts of various anions in CH_3CN–H_2O (1 : 1, v/v). Only an ATP-induced large change in emission was observed although pyrophosphate and ADP perturbed the emission of **2** moderately. Fig. S23 (ESI†) represents the change in emission of **2** with ATP and ADP. Other phosphate anions except pyrophosphate brought about a marginal change (Fig. S19 and S20, ESI†).

UV-vis spectra of both **1** and **2** with phosphate anions in CH_3CN–H_2O (1 : 1, v/v) showed negligible change and intimated their weak interactions. Binding constant values, as determined by the Benesi–Hilderband plot using emission data,[13] are depicted in Table 4. It is clearly indicated that the macrocycle **2** binds ATP and ADP more strongly than the open structure **1**. We believe that this is due to strong chelation of the phosphate group of ATP and ADP into the organized binding centre of the macrocycle **2**.

The interaction of **1** with ATP/ADP was monitored using ^{1}H NMR in DMSO-d_6. The signal at 10.24 ppm that pertains to the –NH groups shifted downfield by 0.56 ppm in the presence of equivalent amounts of ADP (dissolved in D_2O). The benzimidazolium and methylene protons showed downfield chemical shifts of 0.09 and 0.11 ppm, respectively. This indicates that the phosphate ion part of ADP interacts at the cavity of the receptor. The upfield chemical shift of the adenine ring protons during interaction signifies the stacking of the adenine ring in between the pendant naphthalene units. Similar findings were observed with ATP. The corresponding changes in chemical shift values are represented in Fig. 15.

Like **1**, macrocycle **2** showed measurable interaction with ADP and ATP under similar conditions. The amide protons that appeared at 10.33 ppm became too broad to detect its accurate position in the presence of both ATP and ADP (Fig. S24, ESI†). The benzimidazolium protons underwent downfield shifts by 0.53 ppm and 0.59 ppm, in the presence of equivalent amounts of ADP and ATP, respectively. Indeed, the change in chemical shift of benzimidazolium protons in **2** is relatively greater than **1**. This is attributed to the tighter association of the phosphate group into the macrocyclic cavity of **2**. In addition, the upfield shift of the adenine ring protons (0.02 to −0.16 ppm) of both ATP and ADP signifies the close contact of the adenine part with the BINOL motif of the receptor.

Table 4 Binding constant (K_a) values for receptor **2**

Anions	Receptor **1** K_a (M^{-1})	Receptor **2** K_a (M^{-1})
ATP	7.15×10^2 M^{-1}	5.09×10^3 M^{-1}
ADP	9.86×10^2 M^{-1}	2.07×10^3 M^{-1}
Pyrophosphate	nd	3.80×10^3 M^{-1}

nd = not determined.

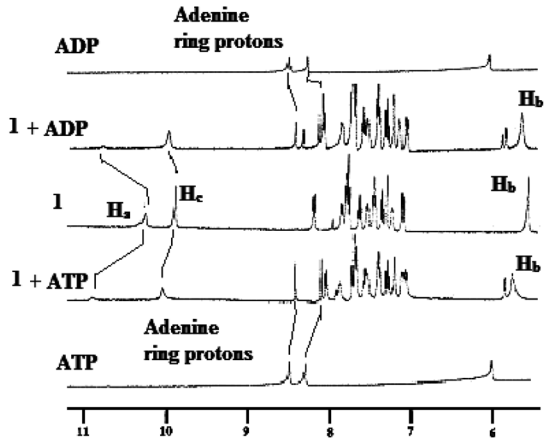

Fig. 15 Partial ^{1}H NMR (DMSO-d_6, 400 MHz) of **1** (c = 2.65 × 10^{-3} M) with equivalent amounts of ATP and ADP [see structure **1** for labeling].

Conclusions

In conclusion, the experimental findings underline the fact that the selective recognition of $H_2PO_4^-$, ADP and ATP by the *ortho*-phenylenediamine-based symmetrical clefts is possible. Due to the interplay of hydrogen bonding and charge–charge interaction while both the receptors **1** and **2** are prone to bind $H_2PO_4^-$ in CH_3CN selectively, in aqueous CH_3CN they exhibit reasonable preference for nucleotide phosphates such as ATP and ADP. Receptor **1** distinguishes ADP from ATP by showing ratiometric change in emission which is unknown in the literature. In contrast, the macrocyclic receptor **2** shows the preferential binding of ATP over ADP.

Experimental

Syntheses

2-(Naphthalen-2-yloxy) ethanol 4a. To a mixture of β-naphthol (4.00 g, 27.5 mmol) and potassium carbonate (5.75 g, 41.62 mmol) in dry acetone (40 mL), 2-chloroethanol (3.35 g, 41.6 mmol) in 5 mL acetone was added dropwise and the reaction mixture was refluxed for 24 h. The reaction mixture was concentrated under vacuum and 30 mL water was added to the mixture. The aqueous layer was extracted with $CHCl_3$ (3 × 100 mL) and dried over anhydrous Na_2SO_4. After the evaporation of solvent in vacuum the crude product was purified by column chromatography using 5% ethyl acetate in petroleum ether as an eluent to give a white crystalline product **4a** (3.50 g,

yield 67%), m.p. 100 °C. ^{1}H NMR (400 MHz, $CDCl_3$): δ 7.77–7.71 (3H, m), 7.44 (1H, t, J = 8 Hz), 7.34 (1H, t, J = 8 Hz), 7.18–7.15 (2H, br m), 4.21 (2H, t, J = 8 Hz), 4.04–4.00 (2H, m), 2.08 (1H, t, J = 4Hz); FTIR (KBr, cm^{-1}): 3368, 2949, 2931, 1629, 1600, 1079. m/z (ES^+): 189.0 $[M + H]^+$.

2-(2-Chloroethoxy)naphthalene 4b. To a stirred solution of **4a** (3.00 g, 15.94 mmol) in $CHCl_3$ (30 mL), $SOCl_2$ (1.4 mL, 19.13 mmol) was added dropwise followed by addition of a catalytic amount of pyridine. The reaction mixture was stirred for 12 h and the solvent was removed under reduced pressure. The residue was neutralized with aqueous $NaHCO_3$ solution and extracted with $CHCl_3$ (3 × 30 mL). The organic layer was dried over anhydrous Na_2SO_4 and concentrated on a rotary evaporator. The crude product was purified by silica gel column chromatography using 2% ethyl acetate in petroleum ether to give pure compound **4b** (3.00 g, yield 91%), m.p. 120 °C. This was directly used in the next step without characterization.

1-(2-(Naphthalen-2-yloxy)ethyl)-1*H*-benzo[*d*]imidazole 5. To a solution of benzimidazole (1.37 g, 11.61 mmol) in dry THF (25 mL), NaH (0.278 mg. 11.61 mmol) was added and refluxed for 1 h under a nitrogen atmosphere. The reaction mixture was then cooled to room temperature and compound **4b** (2.0 g, 9.68 mmol) in dry THF (15 mL) was added followed by addition of tetrabutylammonium iodide (catalytic amount). Reflux was continued for a further 10 h. After completion of the reaction, THF was removed, water was added and the crude mass was extracted with $CHCl_3$ (3 × 30 mL). The organic layer was dried over anhydrous Na_2SO_4 and concentrated on a rotary evaporator. Purification of the crude mass by silica gel column chromatography using 20% ethyl acetate in petroleum ether yielded compound **5** (2.4 g, yield 86%), m.p. 120 °C. ^{1}H NMR (400 MHz, $CDCl_3$): δ 8.07 (1H, s), 7.81 (1H, d, J = 8 Hz), 7.73 (2H, t, J = 8 Hz), 7.66 (1H, d, J = 8 Hz), 7.50 (1H, d, J = 8 Hz), 7.41 (1H, t, J = 8 Hz), 7.35–7.27 (3H, m), 7.10–7.06 (2H, m), 4.63 (2H, d, J = 8 Hz), 4.42 (2H, t, J = 8 Hz); ^{13}C NMR (100 MHz, $CDCl_3$): δ 155.8, 143.8, 143.5, 134.28, 133.8, 129.7, 129.2, 127.7, 126.7, 126.6, 124.0, 123.0, 122.2, 120.5, 118.5, 109.5, 106.7, 66.0, 44.3; FTIR (KBr, cm^{-1}): 3050, 2931, 1627, 1601, 1510, 1257, 1218. m/z (ES^+): 288.2 $[M + H]^+$.

Receptor 1. To a stirred solution of **3** (0.256 g, 0.98 mmol) in CH_3CN, compound **5** (0.848 g, 2.94 mmol) in CH_3CN (10 mL) was added. The reaction mixture was refluxed with stirring for 5 days under a nitrogen atmosphere. After completion, the reaction mixture was cooled to room temperature and filtered. The precipitate was washed with CH_3CN several times to give pure dichloride salt **6** (0.700 g, yield 64%). The dichloride salt **6** (0.92 g, 0.11 mmol) was dissolved in 2 mL hot DMF and NH_4PF_6 (0.056 g, 0.34 mmol) was added to it in one portion. After stirring the reaction mixture for 30 min water was added. The precipitate was filtered, and washed with water and dried to give **1** (0.105 g, yield 90%), m.p. 142 °C. ^{1}H NMR (400 MHz, DMSO-d_6): δ 10.19 (2H, s), 9.88 (2H, s), 8.19 (2H, d, J = 8 Hz), 7.85–7.74 (8H, m), 7.63 (2H, t, J = 8 Hz), 7.52 (2H, t, J = 8 Hz), 7.45 (4H, t, J = 8 Hz), 7.36–7.30 (4H, m), 7.24 (2H, br s), 7.09 (2H, dd, J_1 = 8 Hz, J_2 = 4 Hz), 5.55 (4H, s), 5.08 (4H, s), 4.56 (4H, s); ^{13}C NMR (100 MHz, DMSO-d_6): δ 163.6, 162.3, 155.3, 143.8, 133.9, 131.5, 130.8, 130.1, 129.3, 128.6, 127.4, 126.6, 126.5, 125.8, 125.1, 123.9, 118.2, 114.0, 113.5, 107.0, 65.3, 49.1, 46.4 (one carbon in the aromatic region is unresolved); FTIR (KBr, cm^{-1}): 3392, 3158, 3100, 1709, 1629, 1601, 1542, 1218; HRMS (TOF MS ES^+): $C_{48}H_{42}N_6O_4PF_6^+$, ($M - PF_6$) requires 911.2904 found 911.4358.

2,2′-(1,1′-Binaphthyl-2,2′-diylbis(oxy))diethanol 8. To a mixture of (*rac*)-BINOL **7** (3.00 g, 10.48 mmol) and K_2CO_3 (4.34 g, 31.43 mmol) in dry acetone (40 mL), 2-chloroethanol (2.53 g, 31.43 mmol) in 5 mL acetone was added dropwise and the reaction mixture was refluxed for 24 h. The reaction mixture was concentrated under vacuum and 30 mL water was added to the mixture. The aqueous layer was extracted with $CHCl_3$ (3 × 40 mL) and dried over anhydrous Na_2SO_4. After evaporation of the solvent in vacuum, the crude product was purified by column chromatography using 5% ethyl acetate in petroleum ether as an eluent to give a white crystalline product **8** (2.6 g, yield 65%), m.p. 108 °C. ^{1}H NMR (400 MHz, $CDCl_3$ containing 1 drop DMSO-d_6): δ 7.93 (2H, d, J = 8 Hz), 7.84 (2H, d, J = 8 Hz), 7.40 (2H, d, J = 8 Hz), 7.30 (2H, t, J = 8 Hz), 7.19 (2H, t, J = 8 Hz), 7.07 (2H, d, J = 8 Hz), 4.19–4.15 (2H, m), 4.00–3.96 (2H, m), 3.57–3.48 (4H, m), 2.44 (2H, t, J = 4 Hz, –OH); FTIR (KBr, cm^{-1}): 3294, 2939, 2875, 1619, 1593, 1259, 1241, 1085, 1056; m/z (ES^+): 375.1 $[M + H]^+$.

2,2′-Bis(2-chloroethoxy)-1,1′-binaphthyl 9. To a stirred solution of **8** (1.00 g, 2.67 mmol) in $CHCl_3$ (30 mL), $SOCl_2$ (0.517 mL, 6.94 mmol) was added dropwise followed by addition of pyridine (2 drops, catalytic amount). The reaction mixture was stirred for 12 h and the solvent was removed under reduced pressure. The residue was neutralized with aqueous $NaHCO_3$ solution and extracted with $CHCl_3$ (3 × 30 mL). The organic layer was dried over anhydrous Na_2SO_4 and concentrated on a rotary evaporator. The crude product was purified by silica gel column chromatography with 2% ethyl acetate in petroleum ether to give pure compound **9** (0.900 g, yield 81%), m.p. 64 °C. ^{1}H NMR (400 MHz, $CDCl_3$): δ 7.96 (2H, d, J = 8 Hz), 7.87 (2H, d, J = 8 Hz), 7.42 (2H, d, J = 8 Hz), 7.37–7.33 (2H, m), 7.23–7.21 (2H, m), 7.12 (2H, d, J = 8 Hz), 4.22–4.09 (4H, m), 3.40–3.36 (4H, m); FTIR (KBr, cm^{-1}): 3053, 2953, 2925, 1621, 1593, 1235, 1046; m/z (ES^+): 311.1 $[M + H]^+$.

2,2′-Bis(2-(1*H*-benzo[*d*]imidazol-1-yl)ethoxy)-1,1′-binaphthyl 10. To a solution of benzimidazole (0.747g, 6.32 mmol) in dry THF (25 mL), NaH (0.151 mg, 6.32 mmol) was added and the reaction mixture was refluxed for 1 h under a nitrogen atmosphere. The reaction mixture was then cooled to room temperature and compound **9** (1.0 g, 2.43 mmol) in THF (15 mL) was added followed by addition of tetrabutylammonium iodide (catalytic amount). Reflux was continued for a further 10 h. After completion of the reaction, THF was removed, water was added and extracted with $CHCl_3$ (3 × 30 mL). The organic layer was dried over anhydrous Na_2SO_4 and concentrated on a rotary evaporator. Purification of the crude mass by silica gel column chromatography using 20% ethyl acetate in petroleum ether yielded compound **10** (0.600 g, yield 42), m.p. 114 °C. ^{1}H NMR (400 MHz, $CDCl_3$); δ 7.95 (2H, d, J = 8 Hz), 7.89 (2H, d, J = 8 Hz), 7.64 (2H, d, J = 8 Hz), 7.36 (2H, t, J = 8 Hz), 7.28 (2H, s), 7.22 (2H, t, J = 8 Hz), 7.08–7.15 (4H, m), 6.97 (2H, t, J = 8 Hz), 6.85 (2H, d, J = 8 Hz), 6.69 (2H, s), 4.12–4.09 (2H, m), 3.83–3.96

(6H, m); ^{13}C NMR (100 MHz, $CDCl_3$): δ 153.0, 143.3, 143.0, 133.7, 133.2, 129.7, 129.4, 128.1, 126.6, 125.1, 124.0, 122.7, 121.8, 119.8, 119.7, 114.6, 109.0, 67.1, 44.2; FTIR (KBr, cm^{-1}): 3054, 2976, 2928, 1619, 1591, 1497, 1272, 1264; *m*/*z* (ES^+): 575.2 $[M + H]^+$.

Macrocycle 2. Compounds **10** (0.150 g, 0.26 mmol) and **3** (0.068 g, 0.26 mmol) were taken in dry CH_3CN (60 mL) and the reaction mixture was refluxed under high dilution conditions for 4 days under a nitrogen atmosphere. The reaction mixture was then cooled to room temperature and the white precipitate was filtered. The precipitate was washed with CH_3CN several times to give pure dichloride salt **11** (0.150, yield 69%). The dichloride salt **11** (0.100 g, 0.12 mmol) without characterization was next dissolved in 5 mL hot CH_3OH and NH_4PF_6 (0.056 g, 0.34 mmol) was added to it in one portion. After stirring the reaction mixture for 30 min water was added. The precipitate was filtered, washed with water and dried to give pure salt **2** (0.110 g, yield 87%); m.p. 216 °C. ^{1}H NMR (400 MHz, DMSO-d_6): δ 10.32 (2H, s), 9.41 (2H, s). 8.02–7.96 (4H, m), 7.74 (2H, m), 7.55–7.46 (4H, m), 7.39–7. 12 (12H, m), 6.63 (2H, d, J = 8 Hz), 4.09–4.65 (4H, br m), 4.42–4.40 (4H, br m), 4.35–4.33 (4H, br m); ^{13}C NMR (100 MHz, DMSO-d_6): 163.5, 152.7, 142.6, 132.4, 130.7, 130.3, 130.0, 129.7, 128.8. 128.0, 126.3, 125.9, 125.0, 124.0, 123.9, 119.3, 115.7, 113.1, 112.9, 67.5, 48.8, 46.7 (two carbons in the aromatic region are unresolved). FTIR (KBr, cm^{-1}): 3385, 3060, 1699, 1619, 1598, 1568, 1238, 1088; HRMS (TOF MS ES^+): $C_{48}H_{40}N_6O_4PF_6^+$, $(M - PF_6)^+$ requires 909.2747 found 908.4184 for $(M - PF_6 - H)^+$.

General procedure of fluorescence titration

Stock solutions of the hosts and guests were prepared in CH_3CN or CH_3CN–H_2O ($CH_3CN : H_2O$ = 1 : 1, v/v) and 2.5 ml of the individual host solution was taken in the cuvette. The solution was irradiated at the excitation wavelength maintaining the excitation and emission slits. Upon addition of guest anions, the change in fluorescence emission of the host was noticed. The corresponding emission values during titration were noted and used for the determination of binding constant values.

General procedure of UV-vis titration

The receptors were dissolved in dry UV grade CH_3CN or CH_3CN–H_2O ($CH_3CN : H_2O$ = 1 : 1, v/v) and taken in the cuvette. Then anions dissolved in dry CH_3CN or CH_3OH–H_2O ($CH_3CN : H_2O$ = 1 : 1, v/v) were individually added in different amounts to the receptor solution. The corresponding absorbance values during titration were noted and used for the determination of binding constant values.

Method for Job's plot

The stoichiometry was determined by the continuous variation method. In this method, solutions of host and guest of equal concentrations were prepared in dry CH_3CN or CH_3CN–H_2O. Then host and guest solutions were mixed in different proportions maintaining a total volume of 3 mL of the mixture. The related compositions for host : guest (v/v) were 3 : 0, 2.8 : 0.2, 2.5 : 0.5, 2.2 : 0.8, 2 : 1, 1.8 : 1.2, 1.5 : 1.5, 1 : 2, 0.8 : 2.2, 0.5 : 2.5, 0.2 : 2.8. All the prepared solutions were kept for 1 h with occasional shaking at room temperature. Then emission and absorbance of the solutions of different compositions were recorded. The concentration of the complex, *i.e.* [HG], was calculated using the equation $[HG] = \Delta I/I_0 \times [H]$ or $[HG] = \Delta A/A_0 \times [H]$ where $\Delta I/I_0$ and $\Delta A/A_0$ indicate the relative emission and absorbance intensities. [H] corresponds to the concentration of pure host. Mole fraction of the host (X_H) was plotted against concentration of the complex [HG]. In the plot, the mole fraction of the host at which the concentration of the host–guest complex concentration [HG] is maximum gives the stoichiometry of the complex.

Acknowledgements

We thank DST, New Delhi, India for providing financial support [project SR/S1/OC-76/2010(G); Date:23.08.2011]. IS thanks CSIR, New Delhi, India for a fellowship.

References

1 (*a*) *Chemical Sensor and Biosensors for Medical and Biological Application*, ed. U. S. Wiley-VCH, Weinheim, Germany, 1998; (*b*) C. F. Mason, *Biology of Freshwater Polution*, Longman, New Work, 2nd edn, 1991; (*c*) P. A. Gale, *Acc. Chem. Res.*, 2006, **39**, 465; (*d*) J. W. Steed, *Chem. Commun.*, 2006, 2637; (*e*) A. P. deSilva, H. Q. N. Gunaratne, T. Gunnlaugsson, A. J. M. Huxley, C. P. McCoy, J. T. Rademacher and T. E. Rice, *Chem. Rev.*, 1997, **97**, 1515.

2 (*a*) Z. Xu, X. Chen, H. N. Kim and J. Yoon, *Chem. Soc. Rev.*, 2010, **39**, 127; (*b*) H. T. Ngo, X. Liu and K. A. Jolliffe, *Chem. Soc. Rev.*, 2012, **41**, 4928.

3 B. Alberts, D. Bray, J. Lewis, M. Raff, K. Roberts and J. D. Watson, *Molecular Biology of the Cell*, Garland Publishing, New York, 3rd edn, 1994.

4 (*a*) J. R. Knowles, *Annu. Rev. Biochem.*, 1980, **49**, 877; (*b*) P. Ritter, *Biochemistry, a foundation; Creation Research Society Quarterly June 1999*, Books/Cole, Pacific Grove, CA, 1996; vol. 36.

5 (*a*) W. N. Lipscomb and N. Strater, *Chem. Rev.*, 1996, **96**, 2375; (*b*) P. Nyron, *Anal. Biochem.*, 1987, **167**, 235; (*c*) T. Tabary and L. Ju, *Immunol. Methods*, 1992, **156**, 55; (*d*) A. Kornberg, *J. Biol. Chem.*, 1988, **263**, 1; (*e*) X. Shen, G. Mizuguchi, A. Hamiche and C. Wu, *Nature*, 2000, **406**, 541; (*f*) P. Mahato, A. Ghosh, S. K. Mishra, A. Shrivastav, S. Mishra and A. Das, *Inorg. Chem.*, 2011, **50**, 4162.

6 (*a*) W. Gong and K. Hiratani, *Tetrahedron Lett.*, 2008, **49**, 5655; (*b*) K. Shin-Ichi, H. Yuichi, K. Namiko and Y. Yumihiko, *Chem. Commun.*, 2005, 1720; (*c*) G. Dian-Shun, L. Zhi-Peng, M. Jian-Ping and H. Ru-Qi, *Tetrahedron Lett.*, 2007, **48**, 1221; (*d*) S. I. Konodo, Y. Hiraoka, N. Kurumatani and Y. Yano, *Chem. Commun.*, 2005, 1720; (*e*) H. Ihm, S. Yun, H. G. Kim, J. K. Kim and K. S. Kim, *Org. Lett.*, 2002, **4**, 2897; (*f*) K. Choi and A. D. Hamilton, *Angew. Chem., Int. Ed.*, 2001, **40**, 3912; (*g*) T. H. Kwon and K. -S. Jeong, *Tetrahedron Lett.*, 2006, **47**, 8539; (*h*) Z. Xu, S. Kim, K. -H. Lee and J. Yoon, *Tetrahedron Lett.*, 2007, **48**, 3797; (*i*) S. Sasaki, D. Citterio, S. Ozawa and K. Suzuki, *J. Chem. Soc., Perkin Trans. 2*, 2001, 2309; (*j*) H. Xie, S. Yi, X. Yang and S. Wu, *New J. Chem.*, 1999, **23**, 1105; (*k*) K. Ghosh, A. R. Sarkar and A. P. Chattopadhyay, *Eur. J. Org. Chem.*, 2012, 1311; (*l*) P. Plitt, D. E. Gross, V. M. Lynch and J. L. Sessler, *Chem.–Eur. J.*, 2007, **13**, 1374.

7 (*a*) Z. Xu, J. Singh, J. Lim, J. Pan, H. N. Kim, S. Park, K. S. Kim and J. Yoon, *J. Am. Chem. Soc.*, 2009, **131**, 15528 and references cited therein; (*b*) A. Ojida, Y. Miyahara, J. Wongkongkatep, S.-I. Tamaru, K. Sada and I. Hamachi, *Chem.–Asian, J.*, 2006, 555; (*c*) C. Bazzicalupi, A. Bencini, A. Bianchi, V. Fusi, C. Giorgi, A. Granchi, P. Paoletti and B. Valtancoli, *J. Chem. Soc., Perkin Trans. 2*, 1997, 775; (*d*) H. Wang and W.-H. Chan, *Org. Biomol. Chem.*, 2008, **6**, 162; (*e*) D. Amilan Jose, S. Mishra, A. Ghosh, A. Shrivastav, S. K. Mishra and A. Das, *Org. Lett.*, 2007, **9**, 1979; (*f*) J. Y. Kwon, N. J. Singh, H. N. Kim, S. K. Kim, K. S. Kim and J. Yoon, *J. Am. Chem. Soc.*, 2004, **126**, 8892;

(*g*) C. Bazzzicalupi, S. Biagini, A. Bencini, E. Faggi, C. Giorgi, I. Matera and B. Valtancoli, *Chem. Commun.*, 2006, 4087; (*h*) K. M. K. Swamy, S. K. Kwon, H. N. Lee, S. M. Shanthakumar, J. S. Kim and J. Yoon, *Tetrahedron Lett.*, 2007, **48**, 8663; (*i*) F. Sancenon, A. B. Descalzo, R. Martinez-Manez, M. A. Miranda and J. Sato, *Angew. Chem., Int. Ed.*, 2001, **40**, 2640; (*j*) Z. Xu, D. R. Spring and J. Yoon, *Chem.–Asian J.*, 2011, **6**, 2114; (*k*) H. Y. Kuchelmeister and C. Schmuck, *Chem.–Eur. J.*, 2011, **17**, 5311; (*l*) A. E. Hargrove, S. Nieto, T. Zhang, J. L. Sessler and E. V. Anslyn, *Chem. Rev.*, 2012, **111**, 6603 and references cited therein; (*m*) K. Ghosh and I. Saha, *New J. Chem.*, 2011, **35**, 1397.

8 (*a*) K. Ghosh, I. Saha and A. Patra, *Tetrahedron Lett.*, 2009, **50**, 2392; (*b*) K. Ghosh and I. Saha, *Tetrahedron Lett.*, 2008, **49**, 4591.

9 N. J. Singh, E. J. Jun, K. Chellappan, D. Thangadurai, R. P. Chandran, I. -C. Hwang, J. Yoon and K. S. Kim, *Org. Lett.*, 2007, **9**, 485.

10 P. A. Gale, J. R. Hiscock, S. J. Moore, C. Caltagirone, M. B. Hursthouse and M. E. Light, *Chem.–Asian. J.*, 2010, **5**, 555.

11 P. Job, *Ann. Chim.*, 1928, **9**, 113.

12 (*a*) P. T. Chou, G. R. Wu, C. Y. Wei, C. C. Cheng, C. P. Chang and F. T. Hung, *J. Phys. Chem. B.*, 2000, **104**, 7818; (*b*) F. Foster and C. A. Fife, *Prog. Nucl. Magn. Reson. Spectrosc.*, 1969, **4**, 1.

13 A. Kovalchuk, J. Bricks, L. G. Reck, K. rurack, B. Schulz, A. Sczmna and H. Weiβhoff, *Chem. Commun.*, 2004, 1946.

14 M. J. Frisch, *et al.*, *PM6 calculation was done by using GAUSSIAN 09 (Revision A.02)*, Gaussian, Inc., Wallingford CT, 2004.

